Inhibition of Akt Signaling by Exclusion from Lipid Rafts in Normal and Transformed Epidermal Keratinocytes

Damien Calay[1,2], Dina Vind-Kezunovic[1], Aurelie Frankart[1], Sylviane Lambert[2], Yves Poumay[2] and Robert Gniadecki[1]

Lipid rafts are cholesterol-rich plasma membrane domains that regulate signal transduction. Because our earlier work indicated that raft disruption inhibited proliferation and caused cell death, we investigated here the role of membrane cholesterol, the crucial raft constituent, in the regulation of the phosphatidylinositol-3 kinase (PI3K)/Akt pathway. Raft disruption was achieved in normal human keratinocytes and precancerous (HaCaT) or transformed (A431) keratinocytes by cholesterol extraction or inactivation with methyl-β-cyclodextrin, filipin III, or 5-cholestene-5-β-ol. Lipid raft disruption did not affect PI3K binding to its main target, the epidermal growth factor receptor, nor its ability to convert phosphatidylinositol 4,5-bisphosphate to phosphatidylinositol 3,4,5-trisphosphate but impaired Akt phosphorylation at the regulatory sites Thr^{308} and Ser^{473}. Diminished Akt activity resulted in deactivation of mammalian target of rapamycin, activation of FoxO3a, and increased sensitivity to apoptosis stimuli. Lipid raft disruption abrogated the binding of Akt and the major Akt kinase, phosphatidylinositol-dependent kinase 1, to the membrane by pleckstrin-homology domains. Thus, the integrity of lipid rafts is required for the activity of Akt and cell survival and may serve as a potential pharmacological target in the treatment of epidermal cancers.

Journal of Investigative Dermatology (2010) **130,** 1136–1145; doi:10.1038/jid.2009.415; published online 7 January 2010

INTRODUCTION

The plasma membrane contains nanometer-large dynamic microdomains enriched in cholesterol, sphingolipids, and gangliosides called ''lipid rafts''. These structures are important regulators of signal transduction (Simons and Ikonen, 1997). Because lipid rafts form spontaneously only in the narrow range of cholesterol concentration, the perturbation of membrane cholesterol disrupts lipid raft integrity and has been used extensively to study their role in signaling pathways. In our previous studies, we have documented that in keratinocytes lipid rafts can aggregate into larger structures that retard lateral mobility of the molecules (Vind-Kezunovic *et al.*, 2008b) and influence membrane geometry (Vind-Kezunovic *et al.*, 2008a). Rafts influence the enzymatic activity of several membrane-associated proteins, including the epidermal growth factor receptor (EGFR), insulin growth factor receptor (IGFR), or Fas (Simons and Toomre, 2000; Hueber *et al.*, 2002). Depletion of cholesterol by methyl-β-cyclodextrin (MBCD) in keratinocytes leads to a ligand-independent, transient activation of EGFR, cell-cycle block, apoptosis, and Fas activation (Gniadecki, 2004; Bang *et al.*, 2005; Lambert *et al.*, 2006).

Several studies have shown that Akt/protein kinase B is a cardinal regulator of cell survival and its pathological increase in activity causes carcinogenesis (Datta *et al.*, 1999; Shaw and Cantley, 2006). Membrane receptors including the ErbB family of surface receptors, IGFRs, or Ras stimulate Akt kinase activity by the phosphatidylinositol 3-kinase (PI3K) (Rodriguez-Viciana *et al.*, 1994; Burgering and Coffer, 1995). PI3K catalyzes the conversion of membrane phosphatidylinositol 4,5-bisphosphate (PI(4,5)P2) to phosphatidylinositol 3,4,5-trisphosphate (PI(3,4,5)P3), to which both Akt and its immediate activator phosphatidylinositol-dependent kinase 1 (PDK-1) bind by pleckstrin-homology (PH) domains (Harlan *et al.*, 1994; McManus *et al.*, 2004). Full activation of Akt requires phosphorylation of Thr^{308} by PDK-1, followed by a second phosphorylation at Ser^{473} (Alessi *et al.*, 1997). Downstream components of the Akt/PI3K signaling cascade include mammalian target of rapamycin (mTOR)/$p70^{S6K}$ pathway (Burnett *et al.*, 1998; Nave *et al.*, 1999) and the

[1]*Department of Dermatology, University of Copenhagen, Bispebjerg Hospital, Copenhagen, Denmark and* [2]*Cell and Tissue Laboratory, URPHYM, Faculty of Medicine, University of Namur, Namur, Belgium*

Correspondence: Robert Gniadecki, Department of Dermatology, University of Copenhagen, Bispebjerg Hospital, Bispebjerg Bakke 23, Copenhagen, NV 2400, Denmark. E-mail: rg01@bbh.regionh.dk

Abbreviations: EGFR, epidermal growth factor receptor; MBCD, methyl-β-cyclodextrin; mTOR, mammalian target of rapamycin; PDK-1, phosphatidylinositol-dependent kinase 1; PH, pleckstrin homology; PI(4,5)P2, phosphatidylinositol 4,5-bisphosphate; PI(3,4,5)P3, phosphatidylinositol 3,4,5-trisphosphate; PI3K, phosphatidylinositol-3 kinase; PLC, phospholipase C; PTEN, phosphatase and tensin homologue deleted on chromosome 10

Received 22 August 2008; revised 1 November 2009; accepted 15 November 2009; published online 7 January 2010

apoptosis-related Forkhead family of transcription factors FoxO, causing their emigration from the nucleus (Bonni *et al.*, 1999; Greer and Brunet, 2005).

Lipid rafts are known to be enriched in PI(4,5)P2 and PI(3,4,5)P3 (Hope and Pike, 1996) and are therefore likely to provide the particularly permissive milieu for the interaction between PDK-1 and Akt. Recent fluorescent resonance energy transfer-based and fluorescence correlation spectroscopy-based studies revealed that Akt is more effectively activated when located in lipid raft-like regions (Gao and Zhang, 2008; Lasserre *et al.*, 2008). We have therefore hypothesized that raft disruption could cause the loss or redistribution of phosphoinositol species in the membrane and affect the membrane targeting binding of PH-domain proteins. Because the dependency of Akt activity of lipid rafts is dependent on both cell type and the nature of the activatory stimulus (Gao and Zhang, 2008), we focused in this study on normal, immortalized, and transformed keratinocytes. This is the first study to provide evidence that Akt colocalizes with the detergent-resistant, lipid raft-like regions of the membrane in keratinocytes and that lipid raft disruption by cholesterol depletion causes rapid Akt inactivation and increases keratinocytes susceptibility to apoptosis.

RESULTS

MBCD depletes membrane cholesterol and induces an abrupt dephosphorylation of Akt, inactivation of mTOR, and nuclear export of FoxO3a

HaCaT cells were treated for different times with MBCD, a water-soluble heptasaccharide that binds cholesterol with high affinity (Ohtani *et al.*, 1989). Our previous data, as well as results shown in Figure 1a, documented the efficacy of MBCD for cholesterol removal in epidermal cells. HaCaT cells contain an elevated basal level of Akt activity in comparison with the nontransformed primary keratinocytes and are therefore especially suitable for Akt inhibition studies (unpublished data). As shown in Figure 1b, treatment with 1% MBCD reduced Akt phosphorylation at its regulatory sites (Thr^{308} and Ser^{473}). Phosphorylation levels could be restored in the cells in which cholesterol was repleted (Figure 1c). Of note, the levels of total Akt decreased in cells treated for >3 hours with MBCD that could be caused by proteolytic degradation of Akt molecules by macroautophagy. Disruption of lipid rafts results in the caspase-independent, autophagic cell death (Poster no. 87, European Life Scientist Organization (ELSO) Meeting, Dresden, Germany; http://www.elso.org/index.php?id=abstrlist2005&lid=334). Levels of phosphorylated mTOR, its downstream target $p70^{S6K}$, and FoxO3a were decreased in response to cholesterol depletion (Figure 1b) and were reversed by cholesterol repletion. The reduced phosphorylation of $p70^{S6K}$ was only observed at the Thr^{389} residue, which is mTOR specific. Accordingly, Akt-dependent translocation of FoxO3a from the nucleus to the cytoplasm was blocked in MBCD-treated cells, resulting in an increased nuclear immunoreactivity of FoxO3a (Figure 1d) and enrichment of nuclear fractions in FoxO3a protein (Figure 1e).

The loss of Akt activity due to cholesterol depletion was not specific to HaCaT keratinocytes but was also seen in non-transformed normal keratinocytes (Figure 1g) and in the human squamous cell carcinoma line A431 (Figure 1f). Treatment with 1% of MBCD caused also a redistribution of FoxO3a similarly to what was seen in HaCaT cells (Figure 1d).

To eliminate the possibility that MBCD treatment affected Akt by other mechanisms than cholesterol depletion, we decreased membrane cholesterol levels by simvastatin, used a specific cholesterol binding agent filipin III (Schnitzer *et al.*, 1994), and destabilized lipid rafts with 5-cholesten-5-β-ol. As shown in Figure 1h, all agents were able with different efficacies to decrease the phosphorylation of Akt and Thr^{389} $p70^{S6K}$. Together with the cholesterol repletion experiment (Figure 1c), the data strongly indicate that the decrease in the activity of Akt and its downstream target proteins are due to cholesterol depletion.

PI3K activity is not affected by cholesterol depletion

Dephosphorylation of Akt and inactivation of mTOR/$p70^{S6K}$ and FoxO3a similar to that observed after MBCD treatment could also be induced by the PI3K inhibitors, wortmannin and LY294002 (Figure 1b). We have therefore hypothesized that cholesterol depletion caused PI3K inactivation. In HaCaT keratinocytes the activity of EGFR is the main determinant of PI3K activity (Figure 2a and unpublished data). However, EGFR is activated rather than inactivated by cholesterol depletion in HaCaT keratinocytes (Lambert *et al.*, 2006). In accordance with that finding, the binding of the p85 regulatory subunit of PI3K to the EGFR was increased, rather than decreased in cholesterol depleted cells (Figure 2b,c), except for the cells that were treated for 5 minutes, in which the p85/EGFR ratio was the same as in DMEM-treated control. To evaluate whether the cholesterol depletion could alter PI3K activity without affecting its binding to EGFR, we measured the PI3K activity directly in cell extracts. In agreement with the immunoprecipitation results, no reduction in the PI3K activity was detected after treatment with MBCD in HaCaT cells (Figure 2d), although a slight decrease occurred in A431 cells after 60 minutes treatment (not shown).

Cholesterol depletion induces nuclear translocation of PDK-1

Because the observed changes in Akt activity could not be explained by inactivation of PI3K, we investigated whether activity of PDK-1 is affected by lipid raft integrity. The activity of PDK-1 is regulated by activatory phosphorylation at Ser^{241}; however, as shown in Figure 3a the amount of PDK-1-P-Ser^{241} in control and MBCD-treated cells was equal, or even slightly increased after 15 and 30 minutes of MBCD. Another regulatory mechanism, described recently, is the redistribution of PDK-1 from membrane to the nucleus. The cytoplasmic-nuclear shuttling of PDK-1 is independent of Ser^{241} phosphorylation status and PDK-1 retains kinase activity within the nucleus (Lim *et al.*, 2003). After 15 minutes of MBCD to induce cholesterol depletion in HaCaT keratinocytes, we observed an enhanced nuclear accumulation of PDK-1 (Figure 3b–d).

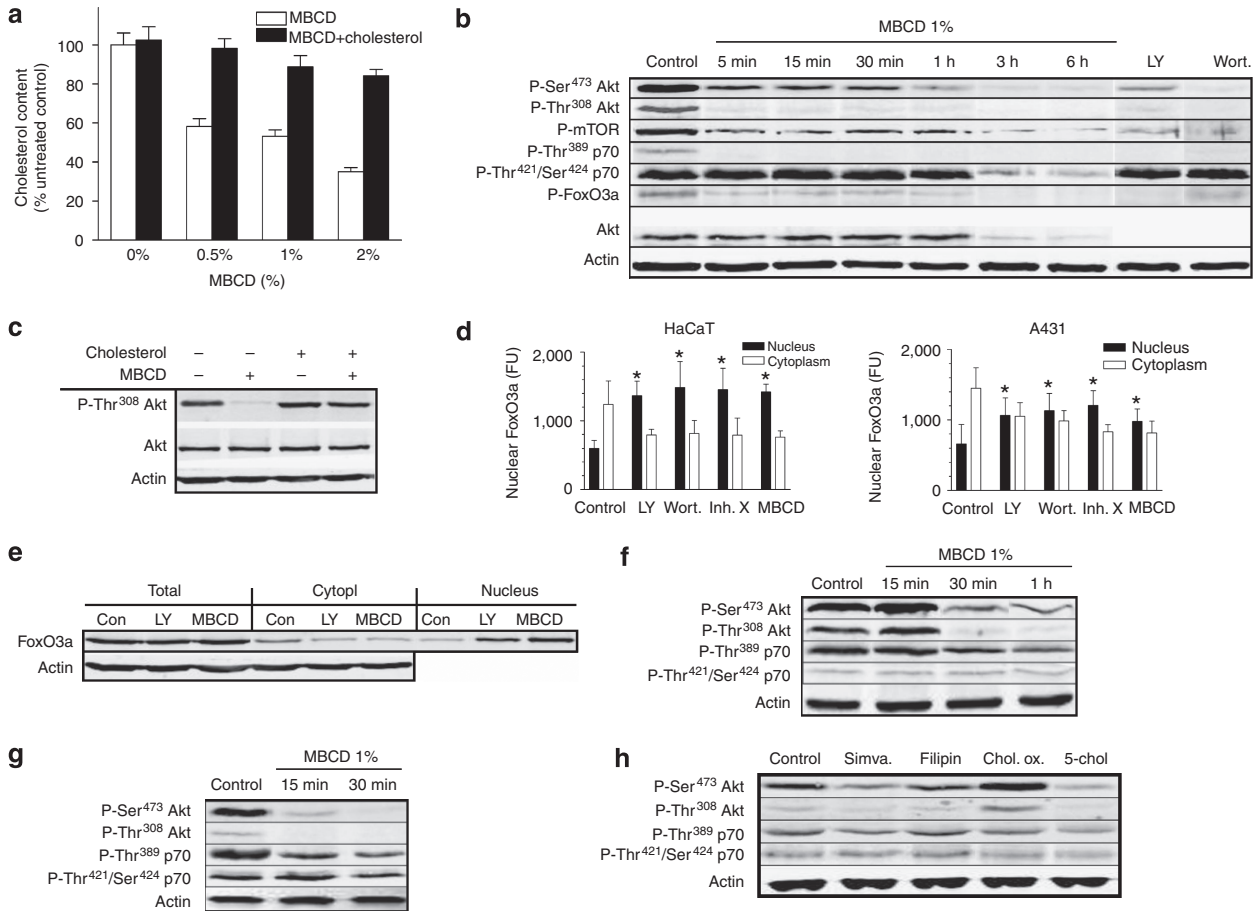

Figure 1. Cholesterol depletion induces dephosphorylation of Akt, mammalian target of rapamycin (mTOR), and translocation of FoxO3a to the nucleus. (**a**) Serum-starved HaCaT cells were treated with methyl-β-cyclodextrin (MBCD) for 15 minutes at indicated concentrations followed by 5 μM cholesterol for a total of 1 hour (solid bars) or serum-free DMEM (open bars). Cholesterol concentration in plasma membrane was determined by cholesterol oxidase Amplex red assay as described in Materials and Methods. Data are mean values ($n=6$ experiments) with SD and represent percentage of the negative control (cells treated only with DMEM). (**b**) Serum-starved HaCaT cells were pretreated with a vehicle (control) or with phosphatidylinositol-3 kinase (PI3K) inhibitors LY294002 (20 μM) or wortmannin (0.5 μM) for 30 minutes at 37 °C before incubation with 1% MBCD in serum-free DMEM for the indicated times at 37 °C. Whole-cell lysates were resolved by SDS–PAGE and immunoblotted with antibodies directed against P-Ser^{473} Akt, P-Thr^{308} Akt, P-mTOR, P-Thr^{389} p70^{S6K}, P-Thr^{421}/Ser^{424} p70^{S6K}, P-FoxO3a, total Akt, and actin (loading control). (**c**) HaCaT cells were cholesterol depleted with 1% MBCD for 15 minutes and then repleted with 5 μM cholesterol (or left in DMEM for control) for an additional 45 minutes, as in **a**. Phosphorylation of Akt, mTOR, and FoxO3a was determined as in **b**. (**d** and **e**) Translocation of FoxO3a to the nucleus in MBCD-treated cells. HaCaT or A431 cells were incubated with LY294002 (20 μM), wortmannin (0.5 μM), Akt inhibitor X (5 μM) or 1% MBCD or left untreated for 30 minutes at 37 °C. Cells were fixed in acetone at 4 °C, rehydrated in phosphate-buffered saline/BSA (0.5%, 15 minutes) and stained with rabbit anti-FoxO3a followed by labeling with secondary Alexa Fluor 488 antibody (both at 4 °C for 30 minutes). Nuclei were counterstained with propidium iodide, outlined, and the FoxO3a-specific fluorescence was determined in the nuclear (black bars) and cytoplasmic (white bars) areas by image analysis of confocal images (**d**). *$P<0.05$, *t*-test against control. (**e**) Nuclear and cytoplasmic fractions from HaCaT cells were prepared as in Materials and Methods and immunoblotted with antibodies against total FoxO3 and actin. (**f** and **g**) Influence of MBCD on Akt/mTOR pathway in A431 cells (**f**) and normal human keratinocytes (**g**). Western blots were performed as in **b**. (**h**) HaCaT cells were incubated with simvastatin (20 μM, overnight), filipin III (2 μM, 1 hour), cholesterol oxidase (Chol. ox., 1 U ml^{-1}, 1 h), 5-cholesten-5-β-ol (5-chol, 5 μM, 2 hours), or with DMSO (vehicle) at 37 °C. Cell lysates were subjected to SDS–PAGE and immunoblotted with the antibodies indicated above.

PI3K, PDK-1, and Akt are excluded from lipid rafts after cholesterol depletion

The nuclear relocalization of PDK-1 raised the possibility that Akt hypophosphorylation on Thr^{308} could result from PDK-1 sequestration outside the enzymatic reaction site in the membrane. If PDK-1-dependent phosphorylation of Akt takes place within the rafts, cholesterol depletion should initially result in the release of both proteins to the nonraft compartment. To investigate whether this takes place, we used approaches based on confocal imaging of PI(3,4,5)P3 and PI(4,5)P2 in HaCaT cells or on the analysis of partitioning of PI3K, PDK-1, and Akt to nonraft heavy fractions and raft-enriched light fractions of the membranes separated according to their buoyant densities. In preliminary experiments, we determined that raft markers, caveolin-1 and flotillin-2, were indeed predominantly detected in light fractions 3 and 4 but partitioned to the heavy fractions in MBCD-treated cells (Figure 4h and data not shown). In control cells, cross-linking of the raft component, the GM1 ganglioside, caused formation of raft clusters resolvable on confocal images as

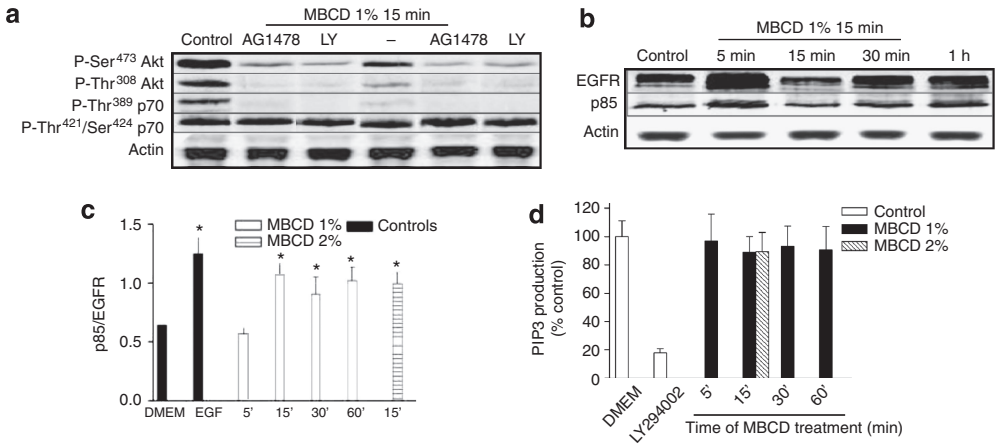

Figure 2. The downregulation of Akt is not due to reduced phosphatidylinositol-3 kinase (PI3K) activity in cholesterol-deprived HaCaT cells. (**a**) Serum-starved HaCaT cells were pretreated with vehicle (control), epidermal growth factor receptor (EGFR) inhibitor tyrphostin AG1478 (1 μM), or the PI3K inhibitor LY294002 (20 μM) for 15 minutes, 37 °C. Subsequently, cells were incubated in the presence or absence of 1% MBCD for an additional 15 minutes at 37 °C. Cell lysates were subjected to SDS–PAGE followed by western blotting for P-Ser473 Akt, P-Thr^{308} Akt, P-Thr^{389} p70^{S6K}, and P-Thr^{421}/Ser^{424} p70^{S6K}. Actin immunoblotting was used as loading control. (**b**) HaCaT cells were treated with or without 1% methyl-β-cyclodextrin (MBCD) in serum-free medium for the indicated times at 37 °C. Cells were lysed, immunoprecipitated with anti-p85 antibodies, and the precipitates resolved by SDS–PAGE and probed with anti-EGFR antibody and anti-p85 PI3K. The actin immunoreactivity was determined in whole-cell lysates to ensure equal amount of total cellular protein for immunoprecipitation. (**c**) Quantification of the ratio of p85 and coimmunoprecipitated EGFR measured from the western blot data ($n = 3$ independent experiments). Cells were treated with DMEM for 5–60 minutes (negative control, graph shows 15-minute value), 10 ng ml^{-1} EGF for 5 minutes (positive control), or were incubated for the indicated times with 1–2% MBCD. *$P < 0.05$ comparing to the negative control, *t*-test. (**d**) HaCaT cells were treated as indicated, immunoprecipitation was performed as described in **b**, and the immune complexes were assayed for their ability to phosphorylate PI(4,5)P2 as a substrate at room temperature during 3 hours. The PI(3,4,5)P3 production was measured by a PI(3,4,5)P3 detector. The PI(3,4,5)P3 production data after treatment with MBCD are depicted as percentages of control (cells incubated in DMEM). *$P < 0.05$ comparing to the control, *t*-test.

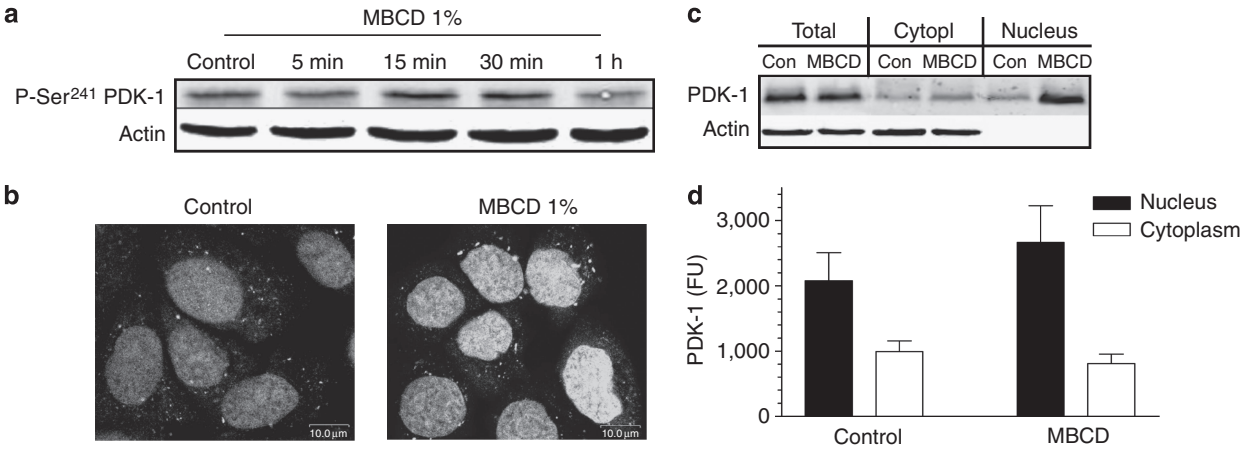

Figure 3. Phosphatidylinositol-dependent kinase 1 (PDK-1) translocates to the nucleus and retains kinase activity in methyl-β-cyclodextrin (MBCD)-treated cells. (**a**) Serum-starved HaCaT cells were treated with or without 1% MBCD for the indicated times at 37 °C. Cell lysates were resolved by SDS–PAGE and immunoblotted with antibody to P-PDK-1. (**b**) Confocal images showing the localization of PDK-1 in serum-starved HaCaT cells incubated in the presence or absence of 1% MBCD for 15 minutes at 37 °C. After fixation, cells were stained with murine anti-PDK-1 antibody followed by the Alexa Fluor 488-conjugated secondary antibody. (**c**) Cells were treated with 1% MBCD for 15 minutes as in **b**. Nuclear and cytoplasmic fractions from the cells were prepared as in Materials and Methods and immunoblotted with antibodies against total PDK-1 and actin. (**d**) Quantification of fluorescence from representative images of cells treated as in **b**. FU, fluorescence units; $n = 20$ cells, means with SD.

CTx^{bright} clusters on the basal, glass-facing portion of the membrane (Figure 4a,c) and on the apical membranes (Figure 4b,d). Immunoreactivities for PI(3,4,5)P3 and PI(4,5,)P2 colocalized with the CTx^{bright} regions. However, this colocalization was lost in the MBCD-treated cells and phosphoinositol staining in these cells was very weak (Figure 4e). Raft cross-linking with the antibody against flotillin 2, an independent raft marker, caused a different pattern comprising formation of smaller, globular domains on the surface of the membrane. Also in this case, flotillin 2 and PI(4,5)P2 and PI(3,4,5)P3 immunoreactivities overlapped in control cells, but not in MBCD-treated cells (Figure 4f,g).

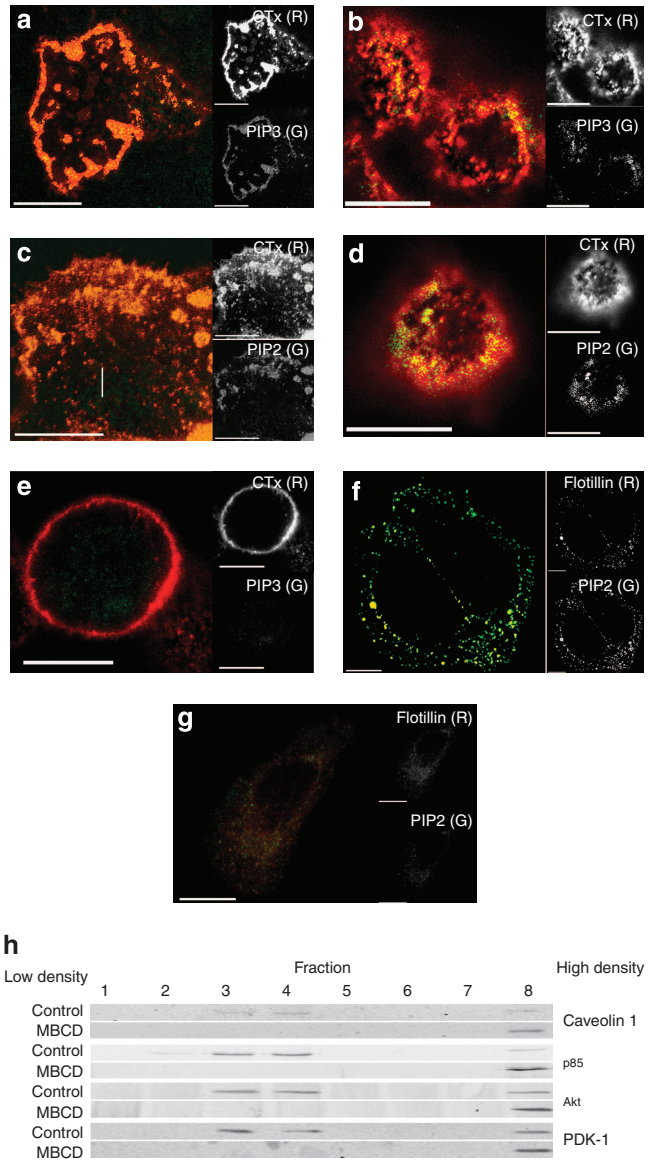

Figure 4. Cholesterol depletion abrogates the association of PI3K, Akt, and PDK-1 with lipid rafts. (**a**–**g**) Confocal images of the cells showing colocalization of PIP3 (**a**, **b**, **e**) and PIP2 (**c**, **d**, **f**, **g**) with lipid raft markers: GM1 ganglioside (stained with cholera toxin B subunit, CTx; **a**–**e**) or flotillin 2 (**f**, **g**). Control cells (**a**–**d** and **f**) or cells treated for 15 minutes with 1% methyl-β-cyclodextrin (MBCD) (**e**, **g**) were preincubated with CTx-Alexa 555 conjugate or anti-flotillin 2 antibody to cross-link lipid rafts. The cells were then fixed in paraformaldehyde, permeabilized in Triton X-100, and incubated with anti-PIP2 or anti-PIP3 antibodies followed by the Alexa 488-conjugated secondary antibodies. Colocalization of markers is reflected by yellow color, black and white images correspond to the individual fluorescence channels, red (R) or green (G). Bar = 10 μm. (**h**) Serum-starved HaCaT cells were treated in the presence or absence of 1% MBCD for 15 minutes at 37 °C. Subsequently cell lysates were subjected to sucrose density gradient centrifugation. Gradients were fractionated and subjected to SDS–PAGE followed by western blotting with antibodies to caveolin-1, p85 subunit of PI3K, total Akt, or PDK-1. Flotation fractions showing enrichment in the raft marker caveolin 1 (i.e., fractions 3 and 4 in our experiments) were designated as raft fractions.

Membrane flotation experiment revealed that PI3K, PDK-1, and Akt were enriched in light fractions, but relocated toward heavy fractions in MBCD-treated cells (Figure 4h). In view of the studies from our laboratory and others (Chen and Resh, 2002) that EGFR is associated with rafts in intact cells, we have considered the possibility that lipid rafts form the nanoscale reaction chambers facilitating the interaction of EGFR, PI3K, PDK-1, and Akt. Because lipid rafts are enriched in phosphoinositides (Hope and Pike, 1996) and both PDK-1 and Akt contain the phosphoinositide-binding PH domains, we determined membrane binding by PH domains in cholesterol-depleted cells.

Inhibition of membrane binding by PH domains in MBCD-treated cells

We used PH domains fused to green fluorescent proteins (GFP) to determine the ability of PH domains to bind to the membrane in living cells. We performed transient transfections in normal keratinocytes and HaCaT cells with Akt-PH-GFP plasmid and phospholipase C (PLC)δ-PH-GFP wild-type (WT) and mutant (MT) constructs (Balla and Varnai, 2002). The PLCδ-PH-GFP^{MT} has a mutated inactivated phosphatidyl-inositol-interacting residue R40L. Both Akt and PLCδ WT PH domains were enriched at the plasma membrane in control cells, but redistributed to intracellular localization after MBCD treatment. This redistribution was rapid and was observable within 5 minutes of MBCD treatment and remained stable over the observation time of 30 minutes. By contrast, the inactivated PLCδ-PH-GFP (MT) remained uniformly distributed throughout the cytoplasm and nucleus without any detectable alteration in fluorescence intensity after MBCD treatment (Figure 5).

Akt inhibition by cholesterol depletion sensitizes the cells to death ligand TRAIL and chemotherapeutic agents etoposid and doxorubicin

The PI3K/Akt signaling pathway is essential in promoting cellular survival (Datta *et al.*, 1999) and has an important role counteracting the pro-apoptotic activity of tumor necrosis factor-related apoptosis inducer ligand (Chen *et al.*, 2001; Thakkar *et al.*, 2001) and chemotherapeutic agents (He *et al.*, 2006). Therefore, we considered the possibility that the inhibitory effect of cholesterol depletion on Akt could enhance TNF-related apoptosis-inducing ligand (TRAIL)-induced apoptosis. As shown in Figure 6, treatment of HaCaT keratinocytes or A431 cells with the apoptosis inducer TRAIL in combination with MBCD, PI3K inhibitors (wortmannin or LY294002), and specific Akt blocker (Akt inhibitor X) resulted in an increased cell death in comparison to treatment with TRAIL alone. The sensitivity of cells to TRAIL in MBCD-treated cells was not further enhanced by PI3K inhibitors, further suggesting that Akt blockade was the primary mechanism after cholesterol depletion and lipid raft disruption. Similar phenomena were observed for etoposid and doxorubicin (Figure 6c–f). The notion that apoptosis was responsible for the observed increased cell death was confirmed by measurements of the effector caspase 3/7 activity (Figure 6g).

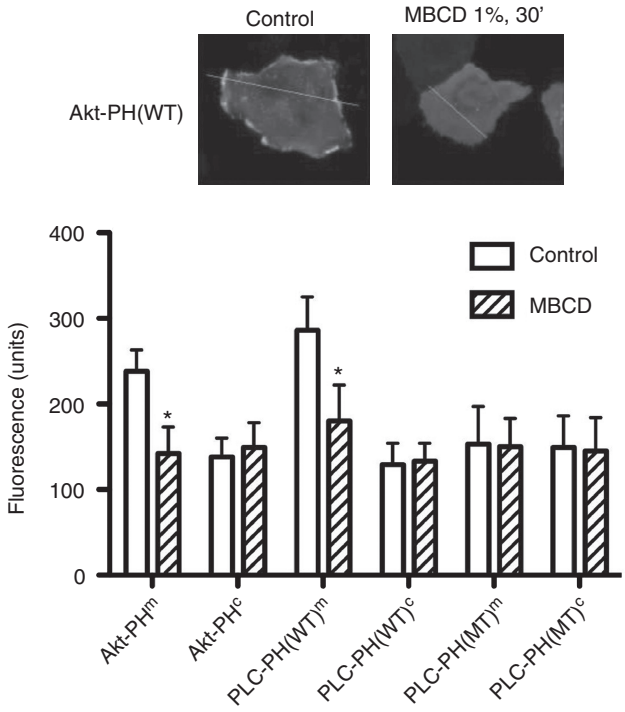

Figure 5. Methyl-β-cyclodextrin (MBCD) induces dissociation of Akt-PH-GFP and PLC-PH-GFP (WT) from the plasma membrane. The cells were transfected with plasmids containing Akt-PH-GFP, PLCδ-PH-GFP(WT), and PLCδ-PH-GFP (MT). Cells were left untreated or treated with 1% MBCD for 0–30 minutes at 37 °C and imaged at room temperature in the phenol red-free DMEM. Control cells were treated with MBCD-free media in identical conditions. Line intensity histograms were obtained from the horizontal cross-sectional images (as marked on the image above) and fluorescence intensity was measured within the membrane (Akt-PH^m, PLC-PH(WT)^m, PLC-PH(MT)^m) and cytoplasmic regions (Akt-PH^c, PLC-PH(WT)^c, PLC-PH(MT)^c) in 50 randomly selected cells. The results of these measurements are shown as mean values in arbitrary fluorescence units with standard deviations ($n = 50$). Open bars, control cells; hatched bars, MBCD-treated cells. *$P < 0.05$ in comparison to the control (*t*-test).

DISCUSSION

The present data indicate that in normal, premalignant, and malignant keratinocytes disruption of cholesterol-enriched lipid rafts in plasma membrane decreases the activity of Akt. Cholesterol perturbation by different agents resulted in an abrupt downregulation of Akt activity and downstream signal transduction to mTOR/p70^{S6K} and FoxO3a. Although similar observations have been independently made on other cell types, including the lymphocytes (Lasserre *et al.*, 2008), breast and prostate cancer cells (Li *et al.*, 2006), and melanoma (Fedida-Metula *et al.*, 2008), this is the first report to show so in normal and transformed keratinocytes and to explain how the activity of Akt is modulated in lipid rafts.

Among different pathways leading to Akt activation (growth factor receptor-dependent activation of PI3K and PDK-1, the integrin-dependent Akt phosphorylation by FAK, and the phosphorylation by nonreceptor kinases Fyn and Src recruited to the E-cadherin-β-/γ-catenin complex at cell–cell junctions (Calautti *et al.*, 2005)), the EGFR/PI3K axis has a dominant role in keratinocytes. However, cholesterol depletion does not cause inactivation of EGFR and did not affect its association with PI3K. Instead, we propose that raft disruption eliminates the phosphoinositide-enriched sites in the membrane to which Akt and PDK-1 bind by PH domains.

We envisage lipid rafts as reaction nanochambers allowing proximity and enzymatic interaction between PDK-1 and Akt. This notion is based on the finding of the copurification of detergent-resistant membrane fractions with Akt. This type of colocalization is not universally found; in most cells Akt is able to reside both inside and outside the rafts and in some cases even preferentially homes to nonraft membrane component (Adam *et al.*, 2007; Arcaro *et al.*, 2007; Gao and Zhang, 2008). Localization of Akt in the rafts may make the keratinocytes particularly sensitive to cholesterol depletion. Cholesterol perturbation causes disruption or dispersion of lipid rafts and movement of the EGFR/PI3K complexes into the more fluid, nonraft areas of the membrane (see also data in Figure 4). In spite of the fact that the activity of PI3K in the cholesterol depleted cells is unchanged, the PI(3,4,5)P3 produced by this enzyme is probably dispersed in the membrane instead of being concentrated in the highly organized raft nanodomains. It is also possible that PI(3,4,5)P3 is preferentially produced in raft regions like shown for the insulin-like growth factor-1 in fibroblasts (Gao and Zhang, 2008). As a consequence, the binding of PH-domain proteins, such as Akt, PLCδ, and PDK-1, to the membrane can be impaired (data in Figure 5), which precludes their spatial interaction and Akt phosphorylation. PDK-1 being unable to dock to the membrane is translocated into the nucleus (Figure 3).

Our results open new venues to the pharmacological inhibition of Akt activity. Akt in keratinocytes constitutes a dominant survival pathway and its blockade leads to apoptotic and autophagic cell death, even in the presence of an active EGFR/ERK axis. The PI3K/Akt/mTOR pathway is hyperactivated in many types of cancer providing survival advantage to transformed cells (Altomare and Testa, 2005) often due to inactivatory mutations in the gene coding phosphatase and tensin homologue deleted on chromosome ten lipid phosphatase mediating dephosphorylation of PI(3,4,5)P3 to PI(4,5)P2. The data presented in this study indicate that cholesterol depletion and Akt inhibition lowers the threshold of sensitivity to death receptor ligands, such as TRAIL, and other chemotherapeutic agents, such as etoposid and doxorubicin. Thus, cholesterol depletion may be a promising method for increasing chemosensitivity to the cytostatics in patients with malignant tumors. Preliminary observations on high-dose statins support this notion (Kornblau *et al.*, 2007).

MATERIALS AND METHODS

Reagents and antibodies

MBCD, cholesterol, water-soluble cholesterol, tyrphostin AG1478, cholesterol oxidase, filipin III, adenosine 5′-triphosphate, doxorubicin and etoposide, and DMSO were purchased from Sigma-Aldrich (St Louis, MO). Simvastatin, LY294002, Akt inhibitor X (10-(4-(*N*-diethylamino)butyl)-2-chlorophenoxazine, HCl),

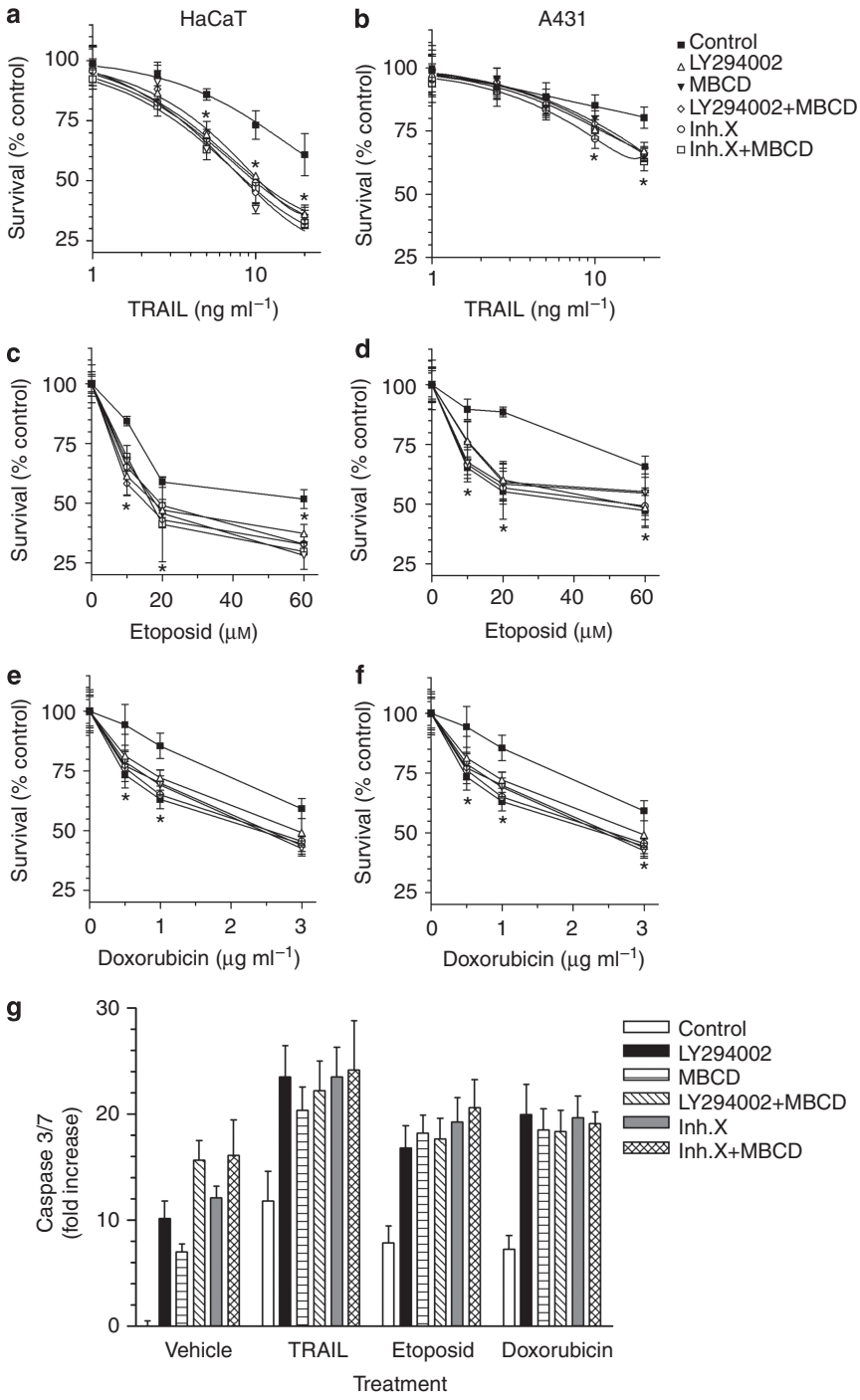

Figure 6. Cholesterol depletion sensitizes HaCaT and A431 cells to the cytotoxic effect of death ligand tumor necrosis factor-related apoptosis-inducing ligand (TRAIL), etoposid, and doxorubicin. (**a**–**f**) HaCaT cells (**a**, **c**, **e**) or A431 cells (**b**, **d**, **f**) were cholesterol-depleted for 15 minutes with 1% methyl-β-cyclodextrin (MBCD) and cultured in the presence of different concentrations of TRAIL, etoposid, or doxorubicin for 24 hours, alone or in combination with Akt inhibitors: LY294002 (20 μM) or Akt inhibitor X (5 μM). To eliminate MBCD-induced toxicity, we removed this compound after total 3 hours incubation. The number of cells was determined by the methylene blue assay. Shown are means with SD. $*P<0.05$, *t*-test. (**g**) HaCaT cells were treated as above and apoptosis was determined after 24 hours using the caspase 3/7 assay as described in Materials and Methods. The following concentrations of apoptosis inducers were used: 5 ng ml^{-1} TRAIL, 20 μM etoposid, and 1 μg ml^{-1} doxorubicin.

and wortmannin were from Calbiochem (La Jolla, CA) and 5-cholestene-5-β-ol was from Steraloids (Newport, RI). Antibodies were purchased from Cell Signaling (Beverly, MA), except for the anti-PI3K p85 subunit (Upstate, Lake Placid, NY); anti-PDK-1 and anti-flotillin 1 (Santa Cruz Biotechnology, Santa Cruz, CA); anti-PI(3,4,5)P3 and anti-PI(4,5)P2 (Echelon Biosciences, Salt Lake City, UT).

The apoptosis inducer Killer TRAIL was from Alexis Biochemicals (San Diego, CA). All other chemicals were obtained from Sigma-Aldrich unless indicated otherwise. Sterols were prepared as 1,000 × solutions in ethanol.

Cell culture, cholesterol depletion, and repletion

HaCaT cell line, a spontaneously immortalized, nontumorigenic cell line derived from human keratinocytes (Boukamp *et al*., 1988) was originally obtained from Dr MR Pittelkow (Mayo Clinic, Rochester, MI). The human epidermoid carcinoma A431 cell line was from the ATCC (Manassas, VA). Cells were maintained in DMEM (Gibco-BRL, Paisley, UK), supplemented with 10% of fetal calf serum (Gibco-BRL), at 37 °C in a humidified incubator containing 5% CO_2. Normal human adult keratinocytes isolated from samples obtained after plastic surgery were seeded into 30 mm Petri dishes at 7×10^3 cells per cm^2 in complete medium (EpiLife containing HKGS; Cascade Biologics, Portland, OR). When cells were approximately 50% confluent, medium was replaced by autocrine growth medium (EpiLife without HKGS) and cells were allowed to reach confluence as described by Jans *et al*. (2004). For cholesterol depletion, the cells were washed in phosphate-buffered saline (PBS) and incubated in serum-free culture media with the indicated concentrations of MBCD, filipin III, simvastatin, or 5-cholestene-5-β-ol. Cholesterol was repleted by incubation with as 5 μM water-soluble cholesterol in DMEM or by cholesterol–cyclodextrin complexes as described by Powers *et al* (2006). In the second method, after the depletion step with MBCD, the cells were washed with PBS and incubated in the absence or presence of cholesterol (Sigma-Aldrich; 80 μg ml^{-1})/1.5 mM MBCD complexes at 37 °C for 15 minutes to replete with cholesterol. Repletion was confirmed by the measurement of total membrane cholesterol (see below).

Western blotting

Cells were grown in 60 mm Petri dishes and allowed to reach 80% confluence. Cells were washed twice with PBS and lysed in 200 μl of sample buffer (0.5 M Tris-HCl (pH 6.8), 5% glycerol, 10% SDS, 0.2 M DTT). Protein concentration was determined in each sample using the D_C reagent (Bio-Rad Laboratories, Hercules, CA) as described by the manufacturer. Total cellular protein (50–100 μg) was separated by SDS–PAGE on 10% gels and electrotransferred onto a nitrocellulose membrane (Bio-Rad Laboratories). The membrane was incubated 1 hours at 4 °C with Li-Cor blocking agent (Lincoln, NE) before incubation with either primary mouse or rabbit antibody overnight at 4 °C. Secondary antibodies labeled with 700IR Dye (anti-mouse) and 800IR Dye (anti-rabbit) (both obtained from Li-Cor) were used for the detection with the infrared Odyssey imaging System (Li-Cor).

Immunoprecipitation

HaCaT cells were seeded in 60 mm Petri dishes and allowed to reach 80% confluence before treatment. Cells were then rinsed once with ice-cold PBS and lysed in 500 μl of RIPA buffer (PBS with 1% Nonidet P-40, 0.5% sodium deoxycholate, 0.1% SDS, complete protease inhibitor (Roche Applied Science, Indianapolis, IN), 1 mM phenylmethylsulfonyl fluoride, 1 mM Na_3VO_4, 50 mM NaF) for 10 minutes at 4 °C. Cells were disrupted by repeated aspiration through a 21-gauge needle, and lysates were transferred to a 1.5 ml centrifuge tube. Cellular debris were pelleted by centrifugation at 10,000 r.p.m. for 10 minutes at 4 °C and the protein concentration of the resulting supernatants was determined using the Bio-Rad D_C reagent. PI3K was precipitated with 5 μl of anti-PI3K p85 subunit antibody overnight at 4 °C with continuous rotation followed by protein G-sepharose (Sigma-Aldrich) for 1 hour at 4 °C. Immunocomplexes were collected by centrifugation for 5 seconds at 14,000*g* at 4 °C, washed three times with ice-cold RIPA buffer, resuspended in 60 μl of electrophoresis sample buffer, and boiled for 5 minutes. The supernatant was analyzed by western blotting, as described above.

PI3K activity

PI3K activity was measured using the PI3 Kinase ELISA kit from Echelon Biosciences following the instructions of the manufacturer. PI3K was isolated from HaCaT or A431 cells by immunoprecipitation as described above and incubated in the presence of ATP and $PI(4,5)P_2$ for 3 hours at room temperature, followed by the $PI(3,4,5)P_3$ detector for 1 hour at room temperature. Reactions were stopped by addition of 0.5 M H_2SO_4 and absorbance was measured at 450 nm.

Membrane cholesterol content

The cholesterol oxidase-Amplex red assay was used using the commercially available kit (Molecular Probes, Portland, OR) according to manufacturer's protocol. Briefly, HaCaT cells were seeded in 24-well plate (120,000 cells per well) and grown for 1 day in DMEM with 10% of fetal calf serum. After the treatment, the cells were washed once with PBS and scraped with the Amplex Red kit buffer. The samples were centrifuged for 10 minutes to pellet the cells and membranes. The concentration of H_2O_2, produced by cholesterol oxidase, was measured in the supernatants by the Amplex red reagent. Cholesterol concentration was determined from the standard curve and adjusted to the total protein concentration in the sample.

DNA constructs and transient transfections

Akt-PH-GFP and PLCδ-PH-GFP (wild-type and R40 L mutant) were originally created by Dr Tamas Balla (National Institute of Child Health and Human Development, National Institutes of Health, Bethesda, MD) (Varnai and Balla, 1998; Balla and Varnai, 2002). NHK were transiently transfected using FuGENE 6 (Roche Applied Science) as recommended by the manufacturer (FuGENE/DNA ratio 3:1). For the transfection of HaCaT cells, 2-day-old cultures were switched to DMEM and transfected using Lipofectamine LTX (Invitrogen, Paisley, UK) according to the manufacturer's protocol. Living cells in phenol-free DMEM medium were imaged using a Leica (Wetzlar, Germany) TCS NT/SP confocal microscope at room temperature using the 488 nm line of an argon laser with a × 63 oil objective. The emission was recorded at 510–555 nm. For each series of experiments, the photomultiplier gain remained unchanged.

Confocal laser scanning microscopy

Cells grown on Lab-Tek chamber slides (Nunc, Roskilde, Denmark) were fixed at 4 °C in either 4% paraformaldehyde for 20 minutes followed by 10 minutes permeabilization in 0.1% Triton X-100 or in acetone for 10 minutes. Cells were rehydrated in PBS with 0.5% BSA (PBS/BSA) for 15 minutes, incubated with the primary rabbit or mouse antibody for 30 minutes at 4 °C, washed twice with PBS, and subsequently labeled with Texas Red anti-rabbit antibody

(Jackson Laboratories, Bar Harbor, ME) or Alexa 488-conjugated anti-mouse antibody (Molecular Probes) antibody for 30 minutes at 4 °C. For double stainings, cholera toxin B subunit (CTx) conjugated with Alexa Fluor 555 (Molecular Probes) was used. The samples were imaged on an Olympus IX70 confocal laser-scanning microscope using the 488 and 568 nm excitation lines from an argon/krypton laser (FluoView Confocal System; Olympus, Tokyo, Japan). Background, nonspecific fluorescence level was determined in samples stained with secondary antibody only. The fluorescence intensity was determined using the proprietary FluoView software in minimum 20 cells for each experiment.

Subcellular fractionation

Cells cultured to 80% confluence in 100 mm Petri dishes were rinsed twice with ice-cold PBS, once with DEB (10 mM Tris-HCl (pH 7.5), 150 mM NaCl) and scraped in 1 ml of TEB (DEB + 1% Triton X-100 and complete protease inhibitor (Roche Applied Science)). Cell lysates were homogenized by repeated aspiration through 23-gauge needles and cleared by centrifugation at 5,000*g*. The pellet was used for the subsequent purification of the nuclei using the Nuclei Isolation EZ Kit (Sigma-Aldrich). The supernatants were either used as cytoplasmic fractions or further processed for the purification of detergent resistant membranes. For the latter, 1 ml of the lysates were adjusted to 40% sucrose and placed at the bottom of an ultracentrifuge tube. A sucrose gradient (30 and 5% in DEB) was then layered and the samples were centrifuged at 39,000 r.p.m. in a Beckman Coulter (Brea, CA) Optima L-80 XP Ultracentrifuge using an SW41 rotor for 18 hours at 2 °C. Fractions of 1.25 ml were collected, diluted in DEB, and subjected to a 41,000 r.p.m. centrifugation using the SW41 rotor for 1 hours at 4 °C. Pellets were recovered and boiled in electrophoresis sample buffer for western blotting.

Cell survival and apoptosis

Cells were seeded on 24-well plates at 100,000 cells per well and allowed to adhere overnight before the treatment. The cells were incubated for 24 hours as indicated, washed twice in PBS, and fixed in 4% buffered paraformaldehyde and stained with 0.1% aqueous methylene blue for 15 minutes. The dye was subsequently extracted with 0.1 M HCl and absorbance was detected at 595 nm (Ultraspec III spectrophotometer; Pharmacia, Uppsala, Sweden). For apoptosis assay, the Caspase-Glo 3/7 Assay (Promega, Madison, WI) detecting the activity of apoptosis-specific caspase 3 and 7 was performed according to the manufacturer's instructions. Luminescence was recorded using a Wallac 1420 Victor II microplate-based luminometer (PerkinElmer, Wellesley, MA).

CONFLICT OF INTEREST

The authors state no conflict of interest.

ACKNOWLEDGMENTS

We are grateful to T. Balla and P. Várnai (Endocrinology and Reproduction Research Branch, National Institute of Child Health and Human Development, National Institutes of Health, Bethesda, USA) for providing the Akt-PH-GFP plasmid. We thank M. Edidin and S. Boyle (Biology Department, The Johns Hopkins University, Baltimore, USA) for kindly providing the PLCδ-PH-GFP constructs with the permission of T. Balla. We thank N. Ninane for excellent technical help with confocal microscopy. We thank E. Hoffmann and I. Petersen for preparation of cell cultures and F. Herpelin and E. Béra for technical assistance. This work was supported by grants from Aage Bangs Foundation and Jeppe Juhl and wife Ovita Juhls Foundation, Denmark, and by grants 1.5033.06 and 2.4506.01 from FNRS and FRFC, Belgium. S.L. holds a fellowship from the FRIA, Belgium.

REFERENCES

Adam RM, Mukhopadhyay NK, Kim J *et al.* (2007) Cholesterol sensitivity of endogenous and myristoylated Akt. *Cancer Res* 76:6238–46

Alessi DR, James SR, Downes CP *et al.* (1997) Characterization of a 3-phosphoinositide-dependent protein kinase which phosphorylates and activates protein kinase Bα. *Curr Biol* 7:261–9

Altomare DA, Testa JR (2005) Perturbations of the AKT signaling pathway in human cancer. *Oncogene* 24:7455–64

Arcaro A, Aubert M, Espinosa del Hierro ME *et al.* (2007) Critical role for lipid raft-associated Src kinases in activation of PI3K-Akt signalling. *Cell Signal* 19:1081–92

Balla T, Varnai P (2002) Visualizing cellular phosphoinositide pools with GFP-fused protein-modules. *Sci STKE* 2002:L3

Bang B, Gniadecki R, Gajkowska B (2005) Disruption of lipid rafts causes apoptotic cell death in HaCaT keratinocytes. *Exp Dermatol* 14:266–72

Bonni A, Brunet A, West AE *et al.* (1999) Cell survival promoted by the Ras-MAPK signaling pathway by transcription-dependent and -independent mechanisms. *Science* 286:1358–62

Boukamp P, Petrussevska RT, Breitkreutz D *et al.* (1988) Normal keratinization in a spontaneously immortalized aneuploid human keratinocyte cell line. *J Cell Biol* 106:761–71

Burgering BM, Coffer PJ (1995) Protein kinase B (c-Akt) in phosphatidylinositol-3-OH kinase signal transduction. *Nature* 376:599–602

Burnett PE, Barrow RK, Cohen NA *et al.* (1998) RAFT1 phosphorylation of the translational regulators p70 S6 kinase and 4E-BP1. *Proc Natl Acad Sci USA* 95:1432–7

Calautti E, Li J, Saoncella S *et al.* (2005) Phosphoinositide 3-kinase signaling to Akt promotes keratinocyte differentiation versus death. *J Biol Chem* 280:32856–65

Chen X, Thakkar H, Tyan F *et al.* (2001) Constitutively active Akt is an important regulator of TRAIL sensitivity in prostate cancer. *Oncogene* 20:6073–83

Chen X, Resh MD (2002) Cholesterol depletion from the plasma membrane triggers ligand-independent activation of the epidermal growth factor receptor. *J Biol Chem* 277:49631–7

Datta SR, Brunet A, Greenberg ME (1999) Cellular survival: a play in three Akts. *Genes Dev* 13:2905–27

Fedida-Metula S, Elhyany S, Tsory S *et al.* (2008) Targeting lipid rafts inhibits protein kinase B by disrupting calcium homeostasis and attenuates malignant properties of melanoma cells. *Carcinogenesis* 8:1546–54

Gao X, Zhang J (2008) Spatiotemporal analysis of differential Akt regulation in plasma membrane microdomains. *Mol Biol Cell* 19:4366–73

Gniadecki R (2004) Depletion of membrane cholesterol causes ligand-independent activation of Fas and apoptosis. *Biochem Biophys Res Commun* 320:165–9

Greer EL, Brunet A (2005) FOXO transcription factors at the interface between longevity and tumor suppression. *Oncogene* 24:7410–25

He YY, Pi J, Huang JL *et al.* (2006) Chronic UVA irradiation of human HaCaT keratinocytes induces malignant transformation associated with acquired apoptotic resistance. *Oncogene* 25:3680–8

Harlan JE, Hajduk PJ, Yoon HS *et al.* (1994) Pleckstrin homology domains bind to phosphatidylinositol-4,5-bisphosphate. *Nature* 371:168–70

Hope HR, Pike LJ (1996) Phosphoinositides and phosphoinositide-utilizing enzymes in detergent-insoluble lipid domains. *Mol Biol Cell* 7:843–51

Hueber AO, Bernard AM, Hérincs Z *et al.* (2002) An essential role for membrane rafts in the initiation of Fas/CD95-triggered cell death in mouse thymocytes. *EMBO Rep* 3:190–6

Jans R, Atanasova G, Jadot M *et al.* (2004) Cholesterol depletion upregulates involucrin expression in epidermal keratinocytes through activation of p38. *J Invest Dermatol* 123:564–73

Kornblau SM, Banker DE, Stirewalt D *et al.* (2007) Blockade of adaptive defensive changes in cholesterol uptake and synthesis in AML by the addition of pravastatin to idarubicin + high-dose Ara-C: a phase 1 study. *Blood* 109:2999–3006

Lambert S, Vind-Kezunovic D, Karvinen S *et al.* (2006) Ligand-independent activation of the EGFR by lipid raft disruption. *J Invest Dermatol* 126:954–62

Lasserre R, Guo XJ, Conchonaud F *et al.* (2008) Raft nanodomains contribute to Akt/PKB plasma membrane recruitment and activation. *Nat Chem Biol* 4:538–47

Li YC, Park MJ, Ye SK *et al.* (2006) Elevated levels of cholesterol-rich lipid rafts in cancer cells are correlated with apoptosis sensitivity induced by cholesterol-depleting agents. *Am J Pathol* 168: 1107–18

Lim MA, Kikani CK, Wick MJ *et al.* (2003) Nuclear translocation of 3′-phosphoinositide-dependent protein kinase 1 (PDK-1): a potential regulatory mechanism for PDK-1 function. *Proc Natl Acad Sci USA* 100:14006–11

McManus EJ, Collins BJ, Ashby PR *et al.* (2004) The *in vivo* role of PtdIns(3,4,5)P3 binding to PDK1 PH domain defined by knockin mutation. *EMBO J* 23:2071–82

Nave BT, Ouwens M, Withers DJ *et al.* (1999) Mammalian target of rapamycin is a direct target for protein kinase B: identification of a convergence point for opposing effects of insulin and amino-acid deficiency on protein translation. *Biochem J* 344(Pt 2):427–31

Ohtani Y, Irie T, Uekama K *et al.* (1989) Differential effects of alpha-, beta- and gamma-cyclodextrins on human erythrocytes. *Eur J Biochem* 186:17–22

Powers KA, Szaszi K, Khadaroo RG *et al.* (2006) Oxidative stress generated by hemorrhagic shock recruits Toll-like receptor 4 to the plasma membrane in macrophages. *J Exp Med* 203:1951–61

Rodriguez-Viciana P, Warne PH, Dhand R *et al.* (1994) Phosphatidylinositol-3-OH kinase as a direct target of Ras. *Nature* 370:527–32

Schnitzer JE, Oh P, Pinney E *et al.* (1994) Filipin-sensitive caveolae-mediated transport in endothelium: reduced transcytosis, scavenger endocytosis, and capillary permeability of select macromolecules. *J Cell Biol* 127:1217–32

Shaw RJ, Cantley LC (2006) Ras, PI(3)K and mTOR signalling controls tumour cell growth. *Nature* 441:424–30

Simons K, Ikonen E (1997) Functional rafts in cell membranes. *Nature* 87:569–72

Simons K, Toomre D (2000) Lipid rafts and signal transduction. *Nat Rev Mol Cell Biol* 1:31–9

Thakkar H, Chen X, Tyan F *et al.* (2001) Pro-survival function of Akt/protein kinase B in prostate cancer cells. Relationship with TRAIL resistance. *J Biol Chem* 276:38361–9

Varnai P, Balla T (1998) Visualization of phosphoinositides that bind pleckstrin homology domains: calcium- and agonist-induced dynamic changes and relationship to myo-[3H]inositol-labeled phosphoinositide pools. *J Cell Biol* 143:501–10

Vind-Kezunovic D, Nielsen CH, Wojewodzka U *et al.* (2008a) Line tension at lipid phase boundaries regulates formation of membrane vesicles in living cells. *Biochim Biophys Acta* 1778:2480–6

Vind-Kezunovic D, Wojewodzka U, Gniadecki R (2008b) Focal junctions retard lateral movement and disrupt fluid phase connectivity in the plasma membrane. *Biochem Biophys Res Commun* 365:1–7